

Metal Halide Perovskite Exciton Tuning Through
Composition Variations and Alloying

Blake Romrell

A senior thesis submitted to the faculty of
Brigham Young University
in partial fulfillment of the requirements for the degree of
Bachelor of Science

John Colton, Advisor

Department of Physics and Astronomy
Brigham Young University

Copyright © 2023 Blake Romrell

All Rights Reserved

ABSTRACT

Metal Halide Perovskite Exciton Tuning Through Composition Variations and Alloying

Blake Romrell

Department of Physics and Astronomy, BYU
Bachelor of Science

Metal halide perovskites are a class of material that has seen a lot of interest over the past two decades as a new material that can be used in LEDs or solar cells. The 2D Ruddlesden-Popper phase of metal halide perovskites, which are more recently of focus, have been investigated for their properties and potential. We measured three samples expected to be Dion-Jacobsen phase perovskites and found them to be not as purely Dion-Jacobsen as believed from their creation. We also investigated how varying the halide in the perovskite changed the energies and if they could be alloyed together. We found that bromide and chloride could be alloyed together continuously to get exciton binding energies and band gap energies between the two pure compositions values, but iodide does not alloy in that way.

Keywords: Metal halide perovskite, Hybrid Organic Inorganic Perovskite, Electroabsorption Spectroscopy

ACKNOWLEDGMENTS

First I want to thank Dr. John Colton, my advisor who made this possible and has been a great help to me in my undergraduate degree. I'm also grateful for the funding from the Brigham Young University College of Physical and Mathematical Science that has supported me, the funding from BYU, as well as NSF funding that has supported the lab and other researchers in the group. The rest of the Colton Lab group during my time here has been helpful in the research efforts and good supports to me, and I'd like to specifically acknowledged the help from Emma McClure, Daniel King, and Sam Jeppson who have helped on this project and data collection, and Michele Eggleston who worked with me on these projects over the summer in the Research Experience for Undergraduates program. Without Kameron Hansen of the University of Utah, I don't think our lab would be working on these projects, and he has helped my understanding of this project a lot, and has produced a majority of samples we have worked on.

Contents

Table of Contents	vii
List of Figures	ix
List of Tables	ix
1 Introduction	1
1.1 Metal Halide Perovskites	2
1.2 Properties To Find	3
1.3 Current Literature on MHPs	4
2 Methods	7
2.1 Electroabsorption procedure	8
2.2 Mathematics Behind the Method	11
3 Results	13
3.1 Halide alloys	14
3.2 Dion-Jacobson Samples	15
3.3 Future work	17
3.4 Conclusion	19
Bibliography	21
Index	23

List of Figures

1.1	Basic Perovskite Structure	2
1.2	Tested efficiency of different Solar cells	5
2.1	Figure of substrate and electrodes	8
2.2	Diagram of lab set-up	9
3.1	Typical EA	13
3.2	Alloy results	15
3.3	Structure of the DJ	16
3.4	OHEPI Wet Absorption	18
3.5	OHEPI Wet EA spectra	18

List of Tables

3.1	Data of some calculated values of DJ and DJ-like samples	17
-----	--------------------------------------------------------------------	----

Chapter 1

Introduction

Metal halide perovskites (MHPs) are a class of semiconductor material of increased interest over the past decade. MHPs can be used to produce LEDs and solar cells, and have a few potential advantages over existing materials being used in these applications, including great increases in efficiency [1–3]. As these materials are more recently being investigated, the models and methods for measuring their properties are less developed than other semiconductor materials. However, if we want to enable good use of MHPs in solar cells or LEDs, understanding their optoelectronic properties is necessary. In the Colton Lab, we have worked on investigating MHPs to further our understanding of the material. We have measured compositions that have not had published measurements, and with our electroabsorption spectroscopy method (to be discussed further in Section 1.2, and Chapter 2) we have made more precise measurements than other published works [4]. In this thesis I will review the different compositions of MHPs we have measured, the exciton properties we have measured from these MHPs, and what we have learned from these measurements.

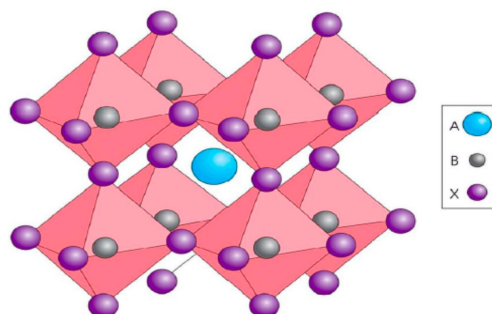


Figure 1.1 The basic perovskite crystalline structure. A is a large organic cation, B is a metal cation, and X is a halogen anion bonded to the metal cation. Adapted from [5].

1.1 Metal Halide Perovskites

Metal halide perovskite describes a class of material with the perovskite crystalline structure. The general form of the perovskite structure can be written as ABX_3 and forms as shown in Fig. 1.1, and in the case of the metal halide perovskites I am discussing here, A is an organic positively charged ion, i.e. an organic cation, B is a metallic cation, and X is a negatively charged ion, i.e. an anion, of a halogen; some use the descriptive term "hybrid organic-inorganic perovskites", which is synonymous, but I will use MHP as the preferred term in this thesis. A large organic molecule can cause MHPs structure to separate into two dimensional layers, which has a significant impact on the properties of the material, compared to organic molecules that allow it to form three dimensional crystals.

This structure lends itself to varying the makeup of MHPs in a several ways, including varying the organic cation, the metal cation, and mixtures of the halide cation in the crystal structure. The organic cation can be varied amongst a number of options, and we have tested phenethyl ammonium (PEA or PE), butyl ammonium (BA), and methyl ammonium (MA), we have tested the metals lead (Pb) and tin (Sn), and the halides have more limited options and we have tested chloride, bromide, iodide, and alloys of pairs of those halides. The results of our measurements and what we learned are topic of this thesis and what will be discussed in the results section. Some of these alloyed

together well, others did not, but their binding and band gap energies are reported in Section 3.1.

1.2 Properties To Find

A key factor of the optoelectronic properties of MHPs come from the properties of excitons that form within their structure. An exciton is a quasi-particle that can form in semiconductor materials when an electron in the valence band is excited to the conduction band. The hole left behind by the excited electron has a positive charge relative to its surroundings, and that electron hole can be considered as a quasi-particle with positive charge. Electron holes can act as charge carriers when they are unbound and free to move within the semiconductor. A positively-charged hole can also be bound to the excited electron that left the hole—bound together in a state comparable to a hydrogen atom, with a single negative and positive charge—and this bound electron-hole pair is the exciton. Certain conditions, like the boundaries of conducting layers spaced with nonconducting organic layers in MHPs, can allow for exciton formation when light with energy higher than the band gap energy is absorbed [6].

An exciton's binding energy will vary from material to material based on both the composition and the layering. The length of the layers of the organic cation, and thus the spacing between crystalline layers, affect the optoelectronic properties. Other properties of interest for an exciton include the radius and effective mass of the exciton. The exciton properties of a semiconductor have an impact on how efficient it can be as a solar cell. Being able to tune the exciton binding energy toward what we want would allow for improving efficiency. Understanding the band-gap energy of the material is also important for the use of MHPs in solar cells and LEDs.

In the Colton Lab we measure these properties using electroabsorption spectroscopy (EA). This is a method that in collaboration with Kameron Hansen [4] we have found to be precise and effective. The method involves scanning through the light spectrum, measuring what proportion of light shone

through that the MHP sample absorbs to get its absorption spectrum. Then the scans are repeated with an applied electric field across the sample. An applied field causes a shift in the spectrum response of the exciton due to the Stark effect, which is that an electric field shifts energy levels of electrons to lower energy dependent on both field strength and the properties of the material, and an oscillation in the band gap area of the spectrum due to the Franz-Keldysh effect [4]. The difference between the absorption with and without an applied electric field can be analyzed to find the band gap energy and the exciton binding energy. With repeated measurements across increasing applied field strengths, we can then find most of the other properties of interest, such as the effective mass and radius of the exciton. For more information on these calculations, and a detailed look at our labs procedures, consult Sam Jeppson's senior thesis.

1.3 Current Literature on MHPs

There is much interest in MHPs as they show a lot of promise as a solar cell material, with efficiencies increasing rapidly to match or beat silicon cells as in Fig. 1.2, and as an efficient, affordable LED material. 3D MHPs have had a lot of interest but have several drawbacks including instabilities with moisture and heat, but 2D MHPs, where there are more distinct separating layers of the organic cation, have had a large increase in publications and interest [1]. The 2D MHPs have higher stability which is great for application in solar cells, but the 2D nature also decreases carrier mobility and causes charge accumulation which undermines performance. In the above source, Chen et al., reviewed and compared the 2D and 3D differences, and a summary of a number of existing 2D measurements, which were largely focused on manipulations of the organic cation. Others have done similar testing, comparing phase pure, and mixed MHPs with different additives [7].

Another method of interest to increase performance is mixing MHPs with other semiconductor materials, like graphene, transition metal disulfides and other materials [2]. These composites

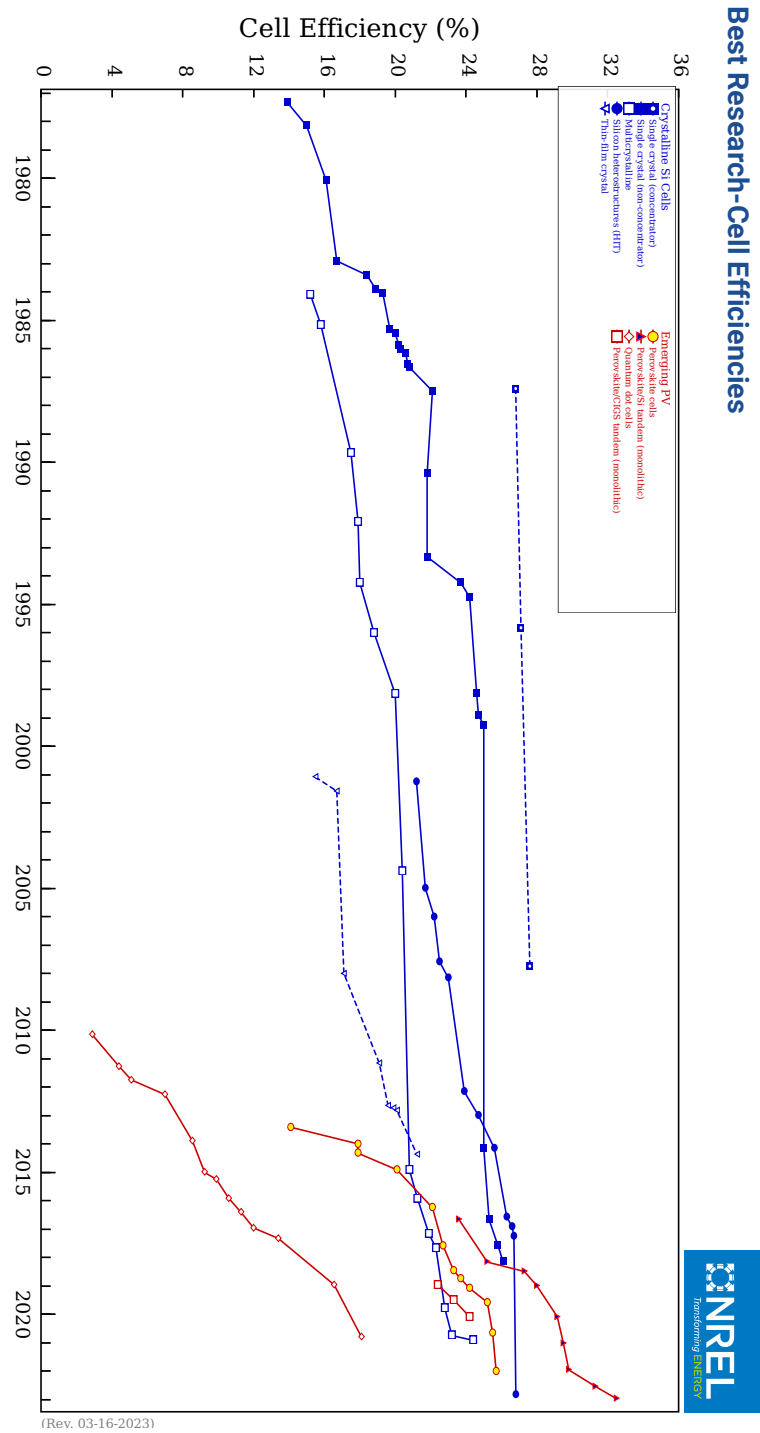


Figure 1.2 A chart of the efficiencies of solar cells of silicon, the current most typical material, compared to perovskites [8].

had better stability, and higher efficiencies than the materials did on their own. Song et al. discussed performance of MHP and MHP compounds in LEDs, solar cells, photo-detectors and other optoelectronic applications [2].

To deal with the issues of stability in air (from various factors such as oxidation) attempting to alter the composition to find more stable but still efficient compounds. Tin is less toxic than lead, which is important for wide-spread use, however tin-based MHPs are less stable. One group, Yun et al. found that when tin fluoride is used, it enhances the stability [9]. Continued investigations like these will help continue the trend we see in Fig. 1.2.

Chapter 2

Methods

Our measurement method for MHPs has primarily been temperature and voltage dependent EA. As discussed in the introduction, the EA spectrum of a material can reveal the properties of the material that can be hard to measure with other standard methods. Another commonly used method for determining the energies requires fitting a line on the slope of the band gap absorption—squared or square-rooted—to extrapolate to the band gap onset energy [4]. We found that extrapolating in that way leads to less accuracy and precision in the measurements than in EA measurements. EA is also able to resolve features in materials with small exciton binding energies, where the features absorption feature are close or overlapping making them hard to resolve using the above described methods, making it a superior method.

To briefly summarize the process before a more detailed discussion below in 2.1, to perform EA you measure the light transmitted through the sample across a spectrum of wavelengths and compare it to light transmitted through a blank to obtain the absorption. Then, an electric field is applied, and the light transmitted is measured again, and from the measured spectrum of light transmitted with an electric field applied, or the electrotransmittance, compared against the normal transmittance and blank we can obtain the EA spectrum. Then by looking at the shape and critical points of the EA spectrum, i.e. zeros and maxima, the band gap and exciton binding energy can be

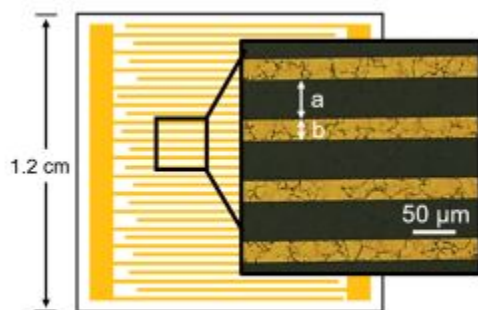


Figure 2.1 An image of an substrate and the electrode dimensions. a is $50 \mu\text{m}$ and b is $30 \mu\text{m}$ Adapted from [10]

accurately determined. A deeper look at the physics and mathematics behind the EA method and how we have utilized it to obtain accurate measurements of properties of interest will be presented in 2.2. For another treatment, that provides step-by-step instructions and a detailed look at the math, I again refer you to look at Sam Jeppson's senior thesis.

2.1 Electroabsorption procedure

Before we can take EA measurements and get into the true first steps for the EA process, I first want to note the preliminary step of sample preparation. The EA measurements are performed on thin films of MHPs deposited on clear substrates with electrodes on them to allow for applying voltages to generate electric fields across the sample. In the Colton Lab we use quartz substrates with gold interdigitated electrodes as shown in Fig. 2.1. The small distances between the electrodes allow for a high field between the electrodes on the sample. We usually do not create the samples; we send the prepared substrates to collaborators, like Kameron Hansen, Wanyi Ni of Los Alamos National Lab, or others we have collaborated with who create the samples and ship them back to us.

Another step that comes before actual measurement is the set up of the optical equipment, as illustrated in 2.2. First the lamp is aligned to shine through a spectrometer that is computer

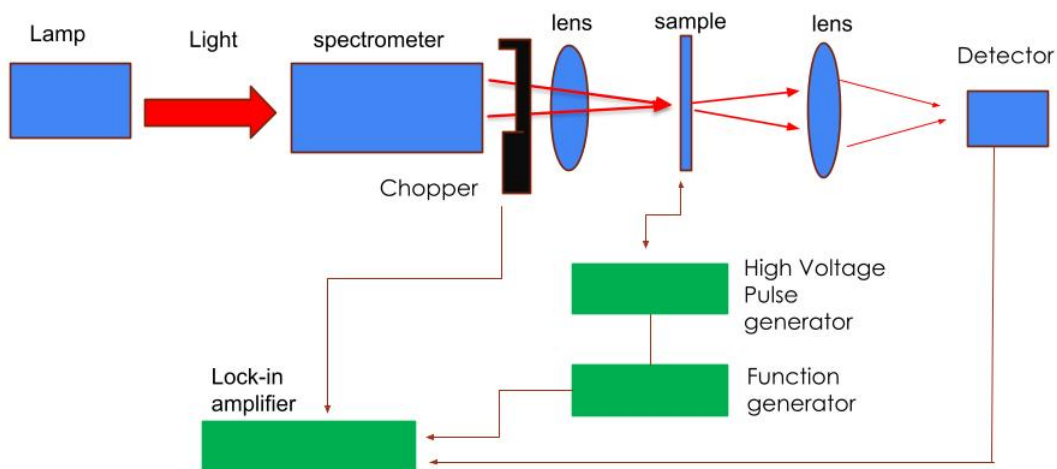


Figure 2.2 A simple diagram of the experimental set-up of our lab.

controlled. At the exit of the spectrometer if the scans are high enough wavelength (for example above 600 nm) a long-pass filter should be inserted to block second order diffraction of lower wavelengths at half the wavelength. Following is an optical chopper, a wheel with slots in it that is motor controlled so the signal can be magnified via a lock-in amplifier. A lock-in amplifier takes an input signal modulated at a reference frequency and uses the orthogonality of sinusoids and integration to select from the input signal only the portion which is at the same frequency, reducing noise and enabling amplification and measurement of small signals. Next on the light path is an iris to control the intensity, and lenses to focus the light onto the sample, which would be mounted on the cold finger of a cryostat. Past that is a lens to focus the light beam onto the final optical element, the detector.

The lamp in the Colton Lab is a xenon arc lamp that is effective in the typical ranges for samples we have measured, from near UV into near IR, and we have used a shop lamp to get better light spectrum in the IR range. The lenses typically are standard lenses; however we sometimes use

fused silica lenses as they can transmit light in the UV whereas glass lenses stop transmitting light near the UV with a sharp onset near 400 nm. The detector used most commonly is a silicon photo-detector, but for samples that are more in the IR range we have used a liquid nitrogen-cooled germanium detector.

Samples are mounted on the cryostat cold finger using GE varnish. The cryostat has leads that can be soldered to the sample's electrodes, but the layer of MHP over the electrode has to be scraped off by a razor so a direct connection can be made. Scans without an applied electric field use the chopper at a frequency around 335 Hz, such that it's not near a multiple of 60 Hz to avoid electrical noise, and the lock-in amplifier is referenced to the chopper. For scans with an applied electric field, the chopper is turned off and positioned to allow light through, and the high voltage generator connected, and the lock-in is referenced to the signal generator triggering the high voltage generator. This is done by moving the cable connection to the lock-in.

The voltage is supplied by a high voltage source capable of 1 kHz frequency pulse waves, triggered by an external function generator, which we set to 983 Hz. The settings we typically use on the spectrometer are an entrance and exit width of 350 microns but it varies based on desired resolution of the scan, and our scan program displays max resolution for a given width enabling easy adjustments. We use a dwell time of three times the lock-in time constant being used. The lock-in time constant is roughly the amount of time the lock-in averages the signal, and the dwell time is how long we wait before taking a measurement. To prevent the measurement being a smoothed step between one data point and another the dwell time has to be longer than the time constant and at least three times is the safe value we use. Typical time constants used are 0.3 s for scans with no electric field and 1 s for scans with an electric field applied.

The first scan performed should be a scan of a blank, a substrate with no MHP on it. Running a scan after all the set-up is simple, as we have a set of LabView programs that control the scan. These LabView programs can be found on GitHub, for the Colton Lab. The important part is knowing

the wavelength range needed to measure. Then a scan of the MHP sample with no applied field, followed by switching to use an applied electric field and scanning again. Initial scans of a sample are often slow as we have to overestimate the range of interest until we've been able to see the EA spectrum and narrow down the range to focus on the features of interest. Usually we will do a series of voltages, repeating the scan with increasing voltage, in ranges from 200 V to 700 V. After scanning at room temperature, we use the cryostat to lower the samples temperature down to 15 K. Then the same process is repeated at low temperature.

A few considerations restrain how we run the scans. At room temperature, the highest voltage is usually lower as we don't want to risk damaging the sample. At low temperature, we don't repeat the blank scan we performed at the beginning as we assume it has not changed, but we do sometimes repeat it at the end to check for drift in the lamp power over time.

After the data has been collected, to analyze it we have to take the recorded spectrums, apply the equations to transform it from transmission to absorption and EA, and plot the spectrums.

2.2 Mathematics Behind the Method

In this section I will present and discuss the equations that describe the EA measurement and analysis method. Look at sources [4, 6, 11] for a more thorough treatment of the topic, and they are the sources where I've gleaned most of this information. Also, as mentioned before, Samuel Jeppson's thesis covers similar material.

The valued of absorption is defined as $A(E)$

$$A(E) = -\log_{10}(T(E)/Tb(E)) \quad (2.1)$$

where E is the energy of the light, and $T(E)$ is the transmittance, and $Tb(E)$ is the transmittance of the blank. EA is the change in absorption, $\Delta A(E)$, where

$$\Delta A(E) = A_{E\text{-field}}(E) - A_{\text{no E-Field}} \quad (2.2)$$

This change results from shifting of charge densities from the applied field, and the Stark effect. For bound states, like the exciton response, the change in energy ΔE can be described in relation to the applied field F , the change in polarizability $\Delta\alpha$ and change in dipole moment $\Delta\mu$

$$\Delta E \propto -\Delta\mu F - \frac{1}{2}\Delta\alpha F^2. \quad (2.3)$$

With a few assumptions a Taylor series expansion can approximate the EA signal ΔA as

$$\Delta A = -\frac{\partial A}{\partial E}\Delta\mu F - \frac{1}{2}\frac{\partial A}{\partial E}\Delta\alpha F^2 + \frac{1}{2}\frac{\partial^2 A}{\partial E^2}(\Delta\mu F)^2. \quad (2.4)$$

In an isotropic material the dipole moments average to zero, and so the first term goes away, and so the EA spectrum should scale according to applied field squared and have the shape of first and second derivatives of the absorption. From a series of scans with increasing applied field, we can then find the polarizability and the dipole moment. The exciton energy can be found from the peak of the no-field absorption spectrum. The band gap energy can be found from the first zero-crossing of the Franz-Keldysh oscillations. The exciton binding energy is the difference between the two.

Chapter 3

Results

One of the sets of samples we tested were variations of the halide, and attempts at alloying pairs of halides in the MHP. We also tested several samples that we thought were Dion-Jacobson phase MHP. The phase of all other samples we have measured has been the Ruddlesden-Popper phase. What that means will be explained and discussed in the section on those samples. In Fig. 3.1 the theoretical idealized model of an absorption spectrum is shown with what it would look like with an applied field overlaid in red. On the right, is the EA spectrum. In both graphs the exciton peak and

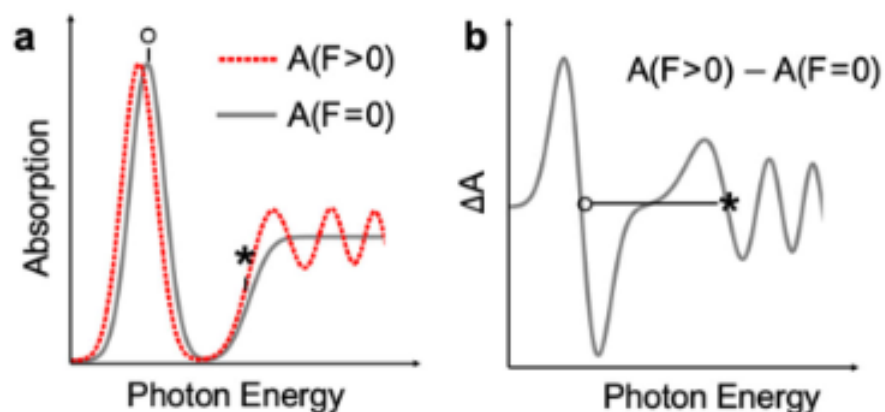


Figure 3.1 Plots of the theoretical standard EA response of a Ruddlesden-Popper phase MHP, both absorption in a and EA in b. The circle is marked at the exciton peak, the asterisk at the band-gap energy. From [12].

the band-gap energies are labeled. In the absorption the shape is that of a narrow, Gaussian-shaped peak on the low energy side (which on a graph where the axis are wavelength the x-axis is flipped, by the $E = hc/\lambda$ relation) and on the right at higher energy you have a slope to the onset of the band-gap absorption. As one could see, it is harder to clearly pinpoint the band-gap even in an idealized model, however in the EA plot these are zero crossings and so can be more accurately determined. The binding energy is then the difference between E_B and E_G which is the length of that line segment connecting them. This demonstrates one aspect of the benefits to the EA spectroscopy method, which we have experimentally found to have higher levels of precision [4] than other methods like the extrapolation discussed previously.

3.1 Halide alloys

We tested various alterations, to see how we might be able to tune the energies of the MHP. As will be demonstrated with discussions of the data below with Fig. 3.2, we found that bromide and chloride can be alloyed in PEA_2PbX_4 where X is the halide or halide mixtures, and mixtures can be made to continuously tune between band gap energies $E_G = 3.425$ and 4.13 eV and exciton binding energies between E_B 349 and 487 meV [13]. Bromide iodide mixtures in PEA_2PbX_4 composition MHPs did not alloy continuously, but were observed to have both $\text{PEA}_2\text{PbBr}_4$ and PEA_2PbI_4 intermixed. This was clear from having two distinct exciton features in their EA response. This would not have been as distinguishable in other methods as the features are close together and so the method using extrapolation from a modified absorption spectrum would struggle with these sorts of samples. Similarly, MHPs with Pb-Sn mixed together did not result in a good alloy, but rather regions of coexisting separate Pb and Sn regions. As with the bromide iodide mixtures, this could be seen with the EA having two exciton features.

For the absorption plots of the bromide chloride, we see an exciton peak at the lower energy side

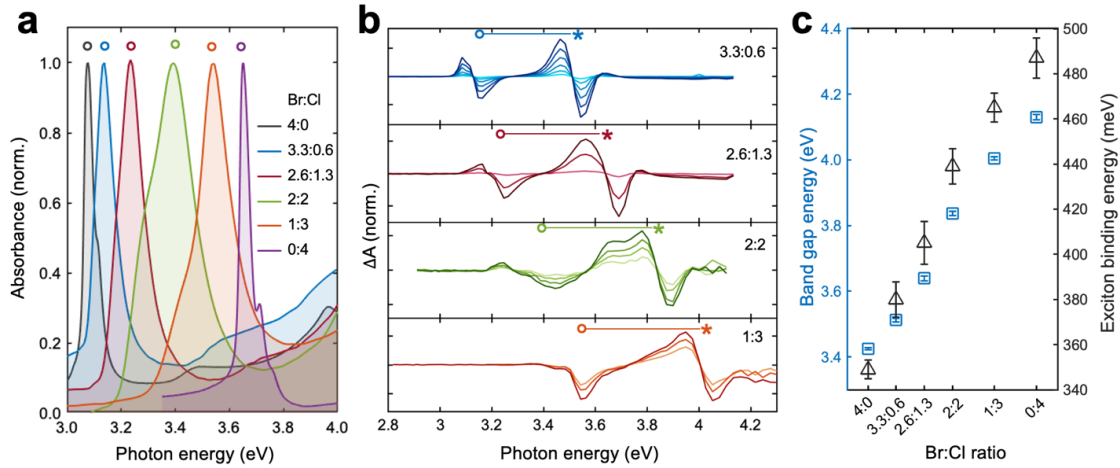


Figure 3.2 Plots of $PEPBr_{4-x}Cl_x$ a: absorption of different levels of alloy, b: EA Voltage series of different levels of alloys. c: E_B and E_G of various levels of alloys. From [12]

where it is pure chloride, and then as the proportion of bromide to chloride increases, the exciton peak shifts over to higher energy, but the movement of the band gap is less clear in the absorption. The EA spectrums are much easier to interpret, with the zero crossings being easy to determine clearly. These plots show show the continual shift of both the exciton and gap energies.

3.2 Dion-Jacobson Samples

The difference between the two phases we have measured samples of is that Ruddlesden-Popper (or RP) phase have two monocationic spacers, and Dion-Jacobson (DJ) phase have one dication per unit of the crystal structure [14]. However, despite our collaborator Wanyi Ni believing she was sending us DJ samples, after collecting EA data for them, we followed up with x-ray diffraction to verify their structure, and found that they were not DJ phase, but some mix of 2D and 3D RP phase as explained below. Their calculated values are displayed below in Table 3.1.

One of the MHP compositions, hexanediammonium (HDA) mixed with lead and iodide in a ABX_4 formula ($HDAPbI_4$) and do form a DJ structure. We found the EA spectrum of $HDAPbI_4$ to

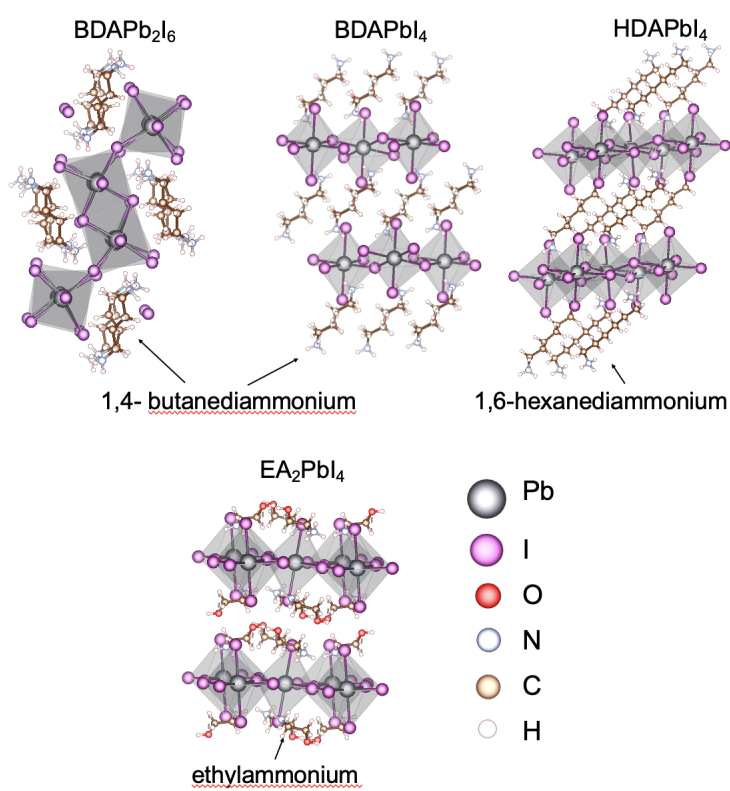


Figure 3.3 Crystal structure of the samples described in this section. From [11].

Table 3.1 Data of some calculated values of DJ and DJ-like samples

Chemical Name	$E_{1s}(15K)$ eV	$E_g(15K)$ eV	$E_b(15K)$ meV
BDAPb ₂ I ₆	2.547 ± 0.003	2.681 ± 0.002	134 ± 4
HDAPbI ₄	2.569 ± 0.004	2.8178 ± 0.003	248 ± 5
BDAPb ₂ Br ₆	3.187 ± 0.003	6.463 ± 0.003	276 ± 4
5F-PEPI	2.485 ± 0.002	2.759 ± 0.002	274 ± 3

be similar to that of BAPI and PEPI that we have measured before.

We were also sent butyldiammonium lead iodide (BDAPb₂I₆ or BDAPbI) , and butyldiammonium lead bromide (BDAPb₂Br₆ or BDAPbBr). These were thought to be of the same type as the HDAPbI₄, but did not actually have a DJ structure. As shown in Fig. 3.3 their structure has touching corners. Some classify them as 3D perovskite due to that geometry; however, these materials' EA response resembles 2D MHPs more than typical 3D MHP values [11]. BDAPbI and BDAPbBr had E_B of 136 and 276 meV respectively, which is much larger than 3D MHP MAPI's value of around 10 meV. Additionally, Wanyi also sent us flourinated PEPI (5F-PEPI), and we found that flourination caused it to have higher E_B than PEPI.

3.3 Future work

In our lab's ongoing work with these samples, we are still working on different MHP compositions. In collaboration with Kelsey Garden of the University of Utah we are investigating OHEPI samples that are able to incorporate water. The dry form has been hard to measure and might not be very crystalline.

The wet version was measured well and Figs. 3.4, 3.5 display the data. The absorption has a clear peak around 550 nm, however the flattening is a little unusual. The different lines of the EA

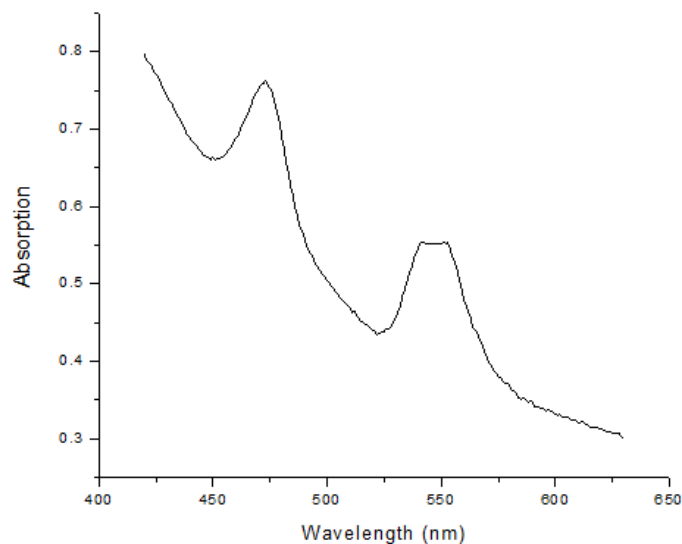


Figure 3.4 The absorption spectrum of water intercalated OHEPI

plot indicate different voltages applied. We have not yet extracted the properties from these plots, as the flattening of the exciton peak and slightly odd features at that position in the EA plot will take more consideration.

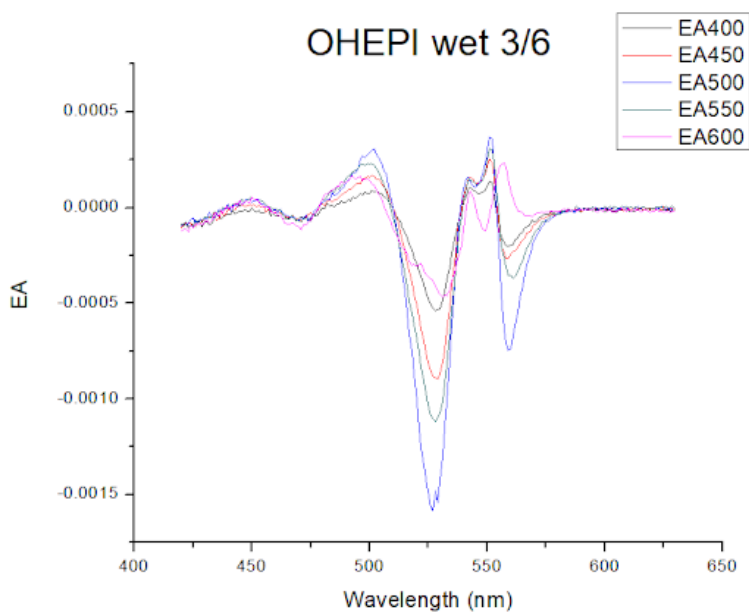


Figure 3.5 The EA spectrum of water intercalated OHEPI. Each line labeled EA### is a different level of voltage applied.

We are also going to investigate MHPs with chiral organic molecules from Azim Haque who Dr. Colton met at NREL, and are going to be measuring the circular dichroism of these materials. Those are scans comparing the response to left and right circular polarized light on the sample and is a different kind of experiment than any we've done recently, but largely uses the same experimental set-up with a few additions. Initial samples of these sort have arrived, but our attempts at using a photo-elastic modulator in our EA experimental set-up is failing, and so we need to troubleshoot our equipment and method.

3.4 Conclusion

Our investigation of MHPs has increased the knowledge of their properties. We measured DJ samples that haven't had many measurements published. Investigations of alloying different metals was found to not yield continuous mixing and tuning of the properties, but distinct areas of one metal or the other. In respect to halide mixtures bromide-iodide mixtures showed the same failure to alloy continuously. However, bromide-chloride as discussed does alloy and its properties taking on values between that of the pure halide MHPs. These findings inform the ability to create MHPs with absorption energies and other optoelectronic properties as desired, to tune their features.

Bibliography

- [1] Y. Chen, Y. Sun, J. Peng, J. Tang, K. Zheng, and Z. Liang, “2D Ruddlesden–Popper Perovskites for Optoelectronics,” *Advanced Materials* **30**, 1703487 (2018), <https://doi.org/10.1002/adma.201703487>; 14.
- [2] T. Song, Q.-X. Ma, Q. Wang, and H.-L. Zhang, “Design of two-dimensional halide perovskite composites for optoelectronic applications and beyond,” *Mater.Adv.* **3**, 756–778 (2022).
- [3] Yukta and S. Satapathi, “Strategies to Enhance Light Emission from Two-Dimensional Perovskite Light-Emitting Diodes: Challenges and Future Opportunities,” *ACS Applied Electronic Materials* **4**, 1469–1484 (2022), doi: 10.1021/acsaelm.1c01142.
- [4] E. Amerling, K. R. Hansen, and L. Whittaker-Brooks, “Resolving buried optoelectronic features in metal halide perovskites via modulation spectroscopy studies,” *J.Mater.Chem.A* **9**, 23746–23764 (2021).
- [5] M. A. Green, A. Ho-Baillie, and H. J. Snaith, “The emergence of perovskite solar cells,” *Nature Photonics* **8**, 506–514 (2014), iD: Green2014.
- [6] G. Lanzani, in *Pump Probe and Other Modulation Techniques, The Photophysics behind Photovoltaics and Photonics* (John Wiley & Sons, Ltd, 2012), Chap. 9, pp. 177–204, <https://onlinelibrary.wiley.com/doi/pdf/10.1002/9783527645138.ch9>.

- [7] A. Caiazzo and R. A. J. Janssen, “High Efficiency Quasi-2D Ruddlesden–Popper Perovskite Solar Cells,” *Advanced Energy Materials* **12**, 2202830 (2022), <https://doi.org/10.1002/aenm.202202830>; 16.
- [8] “Best research cell efficiency,” <https://www.nrel.gov/pv/cell-efficiency.html> .
- [9] K.-R. Yun, T.-J. Lee, S.-K. Kim, J.-H. Kim, and T.-Y. Seong, “Fast and Highly Sensitive Photodetectors Based on Pb-Free Sn-Based Perovskite with Additive Engineering,” *Advanced Optical Materials* **11**, 2201974 (2023), <https://doi.org/10.1002/adom.202201974>; 14.
- [10] C. E. McClure and J. Colton, “Dielectric spectroscopy on 2D and 3D metal halide perovskites using an interdigitated electrode geometry;”.
- [11] K. R. Hansen, Ph.D. thesis, University of Utah, 2022.
- [12] K. R. Hansen, B. Romrell, C. E. McClure, M. Eggleston, A. Barzensky, J. Lin, L. Whittaker-Brooks, and J. S. Colton, “Ruddlesden-Popper Perovskite Alloys: Continuous and Discontinuous Tuning of the Electronic Structure,” Under Review .
- [13] K. R. Hansen *et al.*, “ $E_g - E_b$ engineering of low-dimensional semiconductors,” Under Review .
- [14] D. Ghosh, D. Acharya, L. Pedesseau, C. Katan, J. Even, S. Tretiak, and A. J. Neukirch, “Charge carrier dynamics in two-dimensional hybrid perovskites: Dion–Jacobson vs. Ruddlesden–Popper phases,” *Journal of materials chemistry. A, Materials for energy and sustainability* **8**, 22009–22022 (2020).

Index

alloys, 14

Electroabsorption, 7, 8, 11

 dependent, voltage, 7

 dependent, temperature, 7

Electroabsorption , 3

electrode design, 8

exciton, 3

MHP

 definition, 2

Phase, Dion-Jacobsen, 13, 15